Spectral Effects of Excitonic Interactions in Disordered Solid Films

Regien G. Stomphorst,*,† Tjeerd J. Schaafsma,† and G. van der Zwan‡,§

Molecular Physics Group, Department of Biomolecular Scieces, Agricultural University Wageningen, Dreijenlaan 3, 6703 HA Wageningen, The Netherlands, and Department of Analytical Chemistry and Applied Spectroscopy, Vrije Universiteit, De Boelelaan 1083, 1081 HV Amsterdam, The Netherlands

Received: November 14, 2000; In Final Form: January 22, 2001

This paper describes the absorbance properties of pigments in disordered films. The fluorescence quenching of pigment systems at low concentrations are usually attributed to the presence of so-called statistical pairs. We show that, if line broadening mechanisms are taken into account such as homogeneous and inhomogeneous broadening and statistical distribution of distances between the pigments, the number of potential quenchers decreases dramatically, because all of these effects lead to an increase of the dipole strength of the lowest excitonic state of a dimer. We also show, on the basis of Monte Carlo calculations on assemblies of pigments, that spectral effects beyond a general broadening of the spectrum will not be observed, even for concentrated systems, where a larger number of these statistical pairs may assumed to be present.

1. Introduction

One of the interesting questions of photosynthesis is how antenna systems are able to keep an excited state from degrading or losing its energy by fluorescence, before the excitation is delivered to the reaction center, where it can effectively be used for initializing electron-transfer reactions.

In natural photosynthetic systems, the chromophores are usually embedded in a protein. One of its effects is that the pigments are held in place at specific positions and orientations. The concentration of chromophores in such systems can be quite high. In LHCII, for instance, with 12 chlorophyll pigments in a box of approximately 4 nm size, the average distance between the pigments ranges from 1 to 2 nm.[1] This amounts to a concentration of ≈0.2 M, whereas concentration quenching in dye[2] and chlorophyll solutions[3,4] starts to play an important role at much smaller concentrations of $10^{-3}-10^{-4}$ M. Nevertheless, LHCII is capable of preserving the excited state on chlorophyll a for periods up to several nanoseconds.[5]

Embedding the pigments in a polymer matrix mimics the protein pigment complexes. These systems can be used profitably to study energy transfer,[6,7] because the clustering behavior that chromophores such as chlorophylls or porphyrins often display in water and organic solvents can be avoided. However, matrixes such as poly(vinyl alcohol) do not influence the relative positions and orientations of the chromophores, whereas in photosynthesis, the proteins do. As a consequence, fluorescence quenching at higher concentrations cannot be avoided.

In these random systems, the mechanism of fluorescence quenching remains fundamentally a mystery.[4,8] It is generally assumed that excitations are transferred to so-called "statistical pairs", excitonically coupled dimers with random relative orientation, by a Förster transfer mechanism and that these dimers somehow avoid fluorescence and back−transfer of the excitation.

Because the initial steps in photosynthesis, the harvesting of light and the subsequent transfer of the excitation to a reaction center, are extremely important in reaching its high overall efficiency, a thorough understanding of the underlying mechanisms would be very helpful in the construction of artificial antenna systems.[9]

In a recent paper, Knox[8] argued that on average a statistical pair has a smaller oscillator strength for the lowest excitonic transition than for the highest, leading to a blue-shifted spectrum for a collection of statistical pairs. This is not observed; in general, the absorption spectrum changes little even for relatively high concentrations, and if larger changes are observed, it is most likely due to ground-state interaction effects at higher concentrations.[10]

In this paper, we argue that the effect is even smaller than Knox calculated, for two reasons: first the inclusion of inhomogeneous broadening as diagonal disorder in the exciton Hamiltonian leads to an increase of the oscillator strength of the lowest excitonic state, even for a completely dark state, and second taking a distribution of positions for the monomer comprising a dimer also has a broadening effect. Together these effects lead to a slightly broadened absorption spectrum and not to a blue-shifted spectrum.

Inclusion of a distribution of distances does, however, point to a possible mechanism for fluorescent concentration quenching. On the basis of the nearest neighbor distribution function derived by Hertz,[11] we argue that around every pigment there is likely to be at least one pigment pair of which the pigments are closer than 1 nm within a sphere determined by the Förster radius R_F. Such a dimer will not likely be a dimer in which the pigments have random orientations, because a more parallel configuration will be favored because of steric hindrance. For chlorophylls, bacteriochlorophylls, and porphyrins, such parallel relative orientations can easily lead to close lying charge transfer (CT) states. Evidence for this can be found in large positive first-order contributions (red shifts) to the Stark spectrum of for instance the special pair in the reaction center or LH antenna systems.[12−14] Although CT states are usually slightly higher in energy than the covalent states because of the "Coulomb

* To whom correspondence should be addressed; E-mail: regien@uuu.chem.vu.nl.
† Agricultural University Wageningen.
‡ E-mail: zwan@chem.vu.nl.
§ Vrije Universiteit.

10.1021/jp004180a CCC: $20.00 © 2001 American Chemical Society
Published on Web 04/04/2001

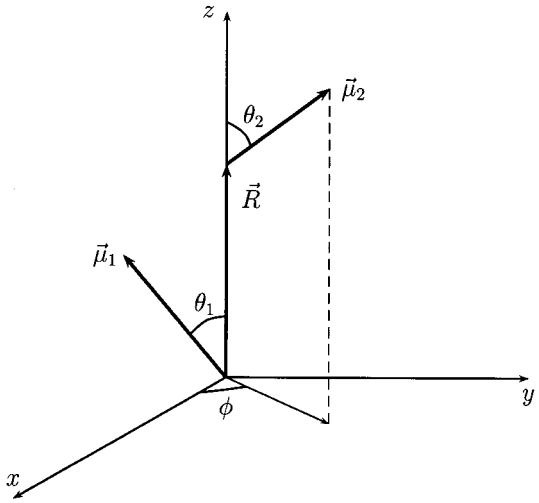

Figure 1. Positions and orientations of the two transition dipole moments in the dimer frame.

penalty", which has to be paid for putting an extra electron on a pigment,[15] in polar media, this is offset by the lowering in energy such a system can get by means of its own reaction field.[16−20] These CT states are obviously dark, because they have no transition dipole moment to the ground state, and for the same reason, they cannot transfer their energy to another chromophore by means of a Förster type transfer mechanism. Hence, they can effectively quench the fluorescence of a concentrated solution of pigments.

In this paper, we present a theoretical study of the absorption spectrum due to excitonic interactions between pigment molecules located at random positions and with random orientation. In the first part of the paper, we will follow Knox[8] and consider dimers only, but we do include inhomogeneous as well as homogeneous broadening and allow for random positions as well. We will give an analytic derivation of Knox's result and show that inclusion of the above broadening mechanisms decrease the blue-shift effect alluded to above. We will also show explicitly that even for a dimer with a dark low excitonic state diagonal disorder will make the lowest transition allowed.

In the second part of the paper, we will consider the absorption spectrum that results if we take a large random collection of pigments. It can then be showed that only a general broadening of the absorption spectrum will be observed at higher concentrations but that even at moderate concentrations a large enough concentration of quenchers is present so that every pigment is close enough to such a quencher to lose its energy by Förster transfer, rather than fluorescence. Observable effects in the absorption spectrum only occur when the pigments get so close that the assumption of random orientations is no longer justified.

2. Description of the System

The dimeric system consists of two two-level monomers, of which we only consider the relative position and orientation of the transition dipole moments. The vector connecting the positions of the transition dipoles is denoted by $\vec{R}$, and we define a dimer frame by letting the *z*-axis point along the $\vec{R}$ direction. Furthermore, we chose the dimer frame such that the transition moment of pigment 1 is in the *xz* plane. The polar angle of pigment 1 is given by θ_1, its azimuth is by definition zero, and the polar angle and azimuth of the transition dipole of pigment 2 are given by θ_2 and ϕ, respectively. The structure is displayed in Figure 1.

The Hamiltonian describing the single excitations of the excitonically coupled dimer is given by the matrix

$$H = \begin{pmatrix} \epsilon_1 & V \\ \mathrm{V} & \epsilon_2 \end{pmatrix} \tag{2.1}$$

The energies ϵ_1 and ϵ_2 are the excitation energies of pigment 1 and pigment 2, respectively, and V is the excitonic interaction

$$V = \frac{1}{4\pi\epsilon_0\epsilon R^3}\vec{\mu}_1\cdot\left(1 - 3\frac{\vec{R}\vec{R}}{R^2}\right)\cdot\vec{\mu}^2 \tag{2.2}$$

Changes in the ground state energy and doubly excited state are neglected throughout this paper. This is justified because $V \ll \epsilon_{1,2}$, and such changes are second order in $V/\epsilon_{1,2}$. The magnitude of the interaction depends on the transition dipole moments and the distance between the pigments. We use the quantity

$$V_0 \approx 5.035\frac{\mu^2}{\epsilon R^3}\ \mathrm{cm}^{-1} \tag{2.3}$$

with μ in D and R in nm, to scale the interactions. For the Q_y transition of chlorophyll for instance, the transition moment is approximately 5.6 D, so that at a distance of 1 nm, the interaction energy V_0 between two chlorophyll molecules is approximately 160 cm^{-1}.

The interaction can furthermore be modified by the relative dielectric constant ϵ, which for most systems is between 1 and 2.

We can now express the interaction energy in terms of the angles defined in Figure 1:

$$V = V_0[\sin\theta_1 \sin\theta_2 \cos\phi - 2\cos\theta_1\cos\theta_2] \tag{2.4}$$

For random systems, the angles θ_1, θ_2, and ϕ and the distance R between the pigments are not fixed but can vary according to a distribution function $N(R, \theta_1, \theta_2, \phi)$. Furthermore, the excitation energies of the monomers are also subject to some variation. For those parts of this paper where we take this diagonal disorder into account, we will assume that these values can be taken from a Gaussian distribution around the unperturbed value ϵ_0, with variance σ. Typical values for σ at room temperature are between 100 and 300 cm^{-1}.[4,6−8]

We are primarily interested in the absorption spectrum of this dimer and the oscillator strength of the lowest excitonic state. It is rather straightforward to diagonalize the Hamiltonian (2.1) and to find the excitonic states and transition moments to these states.[21] The eigenvalues are

$$\epsilon_\pm = \frac{1}{2}[\epsilon_1 + \epsilon_2 \pm \sqrt{(\epsilon_1 - \epsilon_2)^2 + 4V^2}] \tag{2.5}$$

We can write the corresponding excitonic states as

$$|+\rangle = c|1\rangle + s|2\rangle \quad \text{and} \quad |-\rangle = -s|1\rangle + c|2\rangle \tag{2.6}$$

where $|i\rangle$ denotes the state where the excitation is on monomer i and $|\pm\rangle$ denote the excitonic states.

The quantities s and c can be found from

$$s = \frac{t}{\sqrt{1+t^2}} \quad \text{and} \quad c = \frac{1}{\sqrt{1+t^2}} \tag{2.7}$$

with

$$t = \frac{\epsilon_2 - \epsilon_1 + \sqrt{(\epsilon_1 - \epsilon_2)^2 + 4V^2}}{2V} \tag{2.8}$$

The transition moments to the excitonic states can then be written as

$$\vec{\mu}_+ = c\vec{\mu}_1 + s\vec{\mu}_+ \quad \text{and} \quad \vec{\mu}_- = -s\vec{\mu}_1 + c\vec{\mu}_2 \tag{2.9}$$

The intensities of the transition are determined by the square of these quantities, under the assumption that the dimer can occur in any orientation with equal probability. We can write these intensities as

$$I_+ = \mu^2[1 + 2sc\cos\theta] \quad \text{and}$$
$$I_- = \mu^2[1 - 2sc\cos\theta] \tag{2.10}$$

with θ, the angle between the original transition moments, given by $\cos\theta = \cos\theta_1 \cos\theta_2 + \sin\theta_1 \sin\theta_2 \cos\phi$.

This gives us the spectrum for every possible orientation and relative position of the pigments. To find the observed spectrum, we have to average this with the distribution functions $N(R, \theta_1, \theta_2, \phi)$ and the distributions of the pigment energies. We will calculate the probability $P(I, \upsilon)$ of finding an intensity I at frequency υ. This quantity can be found from the expression

$$P(I, \upsilon) = \frac{1}{2}\int_0^\infty \mathrm{d}R \int_{-1}^1 \mathrm{d}\cos\theta_1 \in \int_{-1}^1 \mathrm{d}\cos\theta_2 \int_0^{2\pi} \times$$
$$\mathrm{d}\phi\, N(R, \theta_1, \theta_2, \phi) \int_{-\infty}^{\infty} \mathrm{d}\epsilon_1 \int_{-\infty}^{\infty} \mathrm{d}\epsilon_2\, f(\epsilon_1)\, f(\epsilon_2) \times$$
$$[\delta(\upsilon - \epsilon_+)\delta(I - I_+) + \delta(\upsilon - \epsilon_-)\delta(I - I_-)] \tag{2.11}$$

The distribution f is given by

$$f(\epsilon) = \frac{1}{\sqrt{2\pi\sigma^2}} \exp[-(\epsilon - \epsilon_0)^2 / 2\sigma^2] \tag{2.12}$$

Equation 2.11 forms the basis of all our calculations. The absorption spectrum can be found as

$$\langle I \rangle_\upsilon \equiv I_\upsilon = \int \mathrm{d}I\, IP(I, \upsilon) \tag{2.13}$$

Homogeneous broadening, the result of the finite lifetime of each state, can be introduced in this description by replacing the $\delta(\upsilon - \epsilon_\pm)$ functions by the desired line profile.

Distribution Functions. The distribution functions we will use are all derived from $N(R, \theta_1, \theta_2, \phi)$. We first write it in the form

$$N(R, \theta_1, \theta_2, \phi) = W(R)\, N_R(\theta_1, \theta_2, \phi) \tag{2.14}$$

where $W(R)\,\mathrm{d}R$ is the probability density for finding the nearest neighbor between R and $R + \mathrm{d}R$ and $N_R(\theta_1, \theta_2, \phi)$ is the probability density for finding a set of angles $(\theta_1, \theta_2, \phi)$, given that the distance of the chromophores is R.

An expression for $W(R)$ was derived by Hertz[11,22] and can be written as

$$W(R) = 4n\pi R^2 \exp[-4/3(n\pi R^3)] \equiv 3\frac{R^2}{R_0{}^3} \mathrm{e}^{-R^3/R_0{}^3} \tag{2.15}$$

where n is the particle density. R_0 (in nm) is related to the molarity M of the pigment concentration by

$$R_0 = \left(\frac{3 \times 10^{24}}{4\pi\, 6.025 \times 10^{23}}\right)^{1/3} \approx 0.73\ \mathrm{M}^{-1/3} \tag{2.16}$$

We can use this to estimate the number of quenchers in a given solution. Let us assume that a pair of pigments can act as a quencher when the distance is smaller than 1 nm. The probability of finding such a pair is given by

$$\int_0^1 \mathrm{d}R\, W(R) = 1 - \mathrm{e}^{-1/R_0{}^3} \tag{2.17}$$

with R_0 in nm. Together with eq 2.16, this means that for a molarity of 10^{-3} approximately 2.5×10^{-3} pigment pairs are found that are closer together than 1 nm.

Energy can be transferred at much lower concentrations, as evidenced by depolarization measurements on pigments in films, which show energy transfer at concentrations of 10^{-6}–10^{-7} M.[6,7,23] This also defines a radius R_F, related to the Förster radius, of a sphere around an excited particle in which other pigment particles must be found to transfer the energy to. It is obvious that at concentrations 10^3 higher than these every excited pigment will at least have a few quenching pairs within its Förster radius. Because these pairs only make a small contribution to the total number of pigments, it is not surprising that effects on the absorption spectrum are small.

The inverse of the indefinite integral $F(R)$ of $W(R)$ is given by

$$R = \left(\frac{3}{4\pi n} \ln \frac{1}{1 - F}\right)^{1/3} \tag{2.18}$$

This makes it simple to generate the distribution $W(R)$ from a distribution of uniform deviates F.[24] We will use this in the simulations in section 4.

The angular distribution $N_R(\theta_1, \theta_2, \phi)$ is more complicated. In general, we can state that for large R all orientations are possible, an assumption used by Knox[8] to calculate the spectra. For shorter distances, it obviously depends on the shape of the molecules what the preferred relative orientations are. For planar molecules like (bacterio)-chlorophylls and porphyrins, a shifted coplanar orientation ("slipped deck of cards") appears to be common.[7] This can be introduced as a restriction on $\theta_1 - \theta_2$, cf. Figure 1, which puts the transition dipoles in more or less parallel planes.

In the next section, we first rederive Knox's result by an analytical procedure.

3. Spectral Profile of Statistical Pairs

In this case, we make a number of additional assumptions. The excitation energies ϵ_i of both pigments are equal to ϵ_0. Furthermore, the distance between the pigments is fixed at some value $\bar{R}$, and for that value, all possible orientations are equally probably. The distribution function for positions and angles then becomes

$$N(R, \theta_1, \theta_2, \phi) = \frac{1}{8\pi}\delta(R - \bar{R}) \tag{3.1}$$

Note, however, that there is no conceivable limit in which eq 2.15 reduces to a delta function, except for the "close packing" situation, in which case the other assumptions are hardly justified and singling out a pair of pigments from the closely packed cluster to calculate the absorption spectrum of the complete systems makes no sense. In other words, we do not expect the absorption spectrum of the complete system to even remotely resemble the absorption spectrum of a collection of random

pairs. The calculation is still useful, because it can provide us with an estimate of the number of potential quenchers for this situation.

In addition, eq 2.5 simplifies to

$$\epsilon_{\pm} = \epsilon_0 \pm V \tag{3.2}$$

and t, eq 2.8, becomes

$$t = \frac{|V|}{V} = \text{sign}(V) \tag{3.3}$$

Finally, R in eq 2.4 has to be replaced by $\bar{R}$.

The absorption intensities reduce to the following expressions:

$$I_{+} = \mu^2[1 + t\cos\theta] \quad \text{and} \quad \mu^2[1 - t\cos\theta] \tag{3.4}$$

The intensities and excitation frequencies of course still depend on all the angles involved in the problem.

Equation 2.11 also becomes simpler:

$$P(I, \upsilon) = \frac{1}{16\pi}\int_{-1}^{1} \mathrm{d}\cos\theta_1 \int_{-1}^{1} \mathrm{d}\cos\theta_2 \int_{0}^{2\pi} \times \mathrm{d}\phi\,[\delta(\upsilon - \epsilon_{+})\delta(I - I_{+}) + \delta(\upsilon - \epsilon_{-})\delta(I - I_{-})] \tag{3.5}$$

In the Appendix, we show that this integral can be evaluated exactly and be expressed in an elliptic function. In the Appendix, we also derive an analytical expression for the function $I(\upsilon)$, which is shown to be equal to

$$I(\upsilon) = \mu^2\left[\frac{1}{2}(\upsilon - \epsilon_0) + (\epsilon_0 + V_0 - \upsilon)\frac{\text{asinh}\sqrt{3}}{2\sqrt{3}}\right] \quad \text{for } |\upsilon - \epsilon_0| < V_0 \tag{3.6}$$

and

$$I(\upsilon) = \mu^2\left[\frac{1}{2}(\upsilon - \epsilon_0) - \frac{\upsilon - \epsilon_0}{|\upsilon - \epsilon_0|}\sqrt{\frac{(\upsilon - \epsilon_0)^2 - {V_0}^2}{3}} + \frac{\epsilon_0 + V_0 - \upsilon}{2\sqrt{3}}\left(\text{asinh}\,\sqrt{3} - \text{asinh}\,\sqrt{\frac{(\upsilon - \epsilon_0)^2}{{V_0}^2} - 1}\right)\right] \quad \text{for } V_0 < |\upsilon - \epsilon_0| < 2V_0 \tag{3.7}$$

In these expressions, the function asinh is the inverse hyperbolic sine.

In Figure 2, we show this spectrum for a pair of chlorophyll a molecules at a distance of $\bar{R} = 1$ nm. It is identical to the one calculated by Knox[8] by Monte Carlo techniques.

The spectrum shown in Figure 2 is in fact built of stick spectra. The effects of homogeneous broadening can be taken into account by dressing the sticks with a Gaussian, or Lorentzian, line shape. In that case, we replace the terms $\delta(\upsilon - \epsilon_{\pm})$ by the appropriate line shape function and subsequently perform the integrations numerically. Homogeneous broadening is related to the lifetime of the chromophores, which for chlorophyll a in solution was measured to be ≈5 ns, and the width of the phonon wing, which is the main contribution. We estimate the homogeneous line width to be 100 cm^{-1}, at room temperature. This has important consequences for a possible quenching mechanism based on these statistical pairs. The dashed spectrum in Figure 2 shows the homogeneously broadened spectrum of statistical pairs.

Quenching is supposed to take place by the following mechanism: an excited monomer loses its energy by the Förster transfer mechanism to a nearby statistical dimer. This cannot be to the lower excitonic state of that dimer because that state is supposed to be dark and thus cannot have a transition dipole moment and can consequently not interact with the monomer. The upper excitonic state of the dimer thus gets excited, within a very short time loses some of its energy through interaction with the surrounding medium, and reduces to the lower excitonic state. If that state is indeed dark, fluorescence will be quenched. Within this context, dark of course means that it will lose its energy some other way, before it has a chance to fluoresce. This is not easy to quantify on the basis of the above picture, but let us assume all states in the lower 10% of the above spectrum are sufficiently dark to act as quenching states. A smaller number will certainly not give enough dimers with the correct geometry in the near neighborhood of our excited pigment, as our calculations of the previous section show.

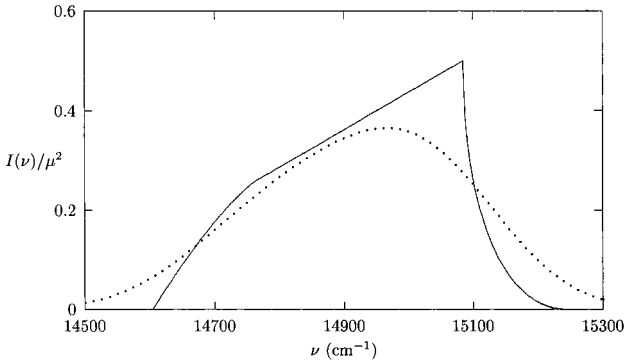

Figure 2. Spectrum of an ensemble of statistical pairs. The properties of the Q_y transition of chlorophyll a pigments were used to model this spectrum. The distance between the pigments is 1 nm, their transition dipole moment 5.6 D, and the transition energy was taken to be 14 925 cm^{-1} (670 nm). The dashed spectrum is obtained by giving every realization a homogeneous width of 100 cm^{-1}.

What is not visible in the above spectrum is that it results from pairs of lines and not from uncorrelated single lines. Moreover, these lines are symmetrical with respect to the unperturbed excitation energy ϵ_0. That means that the upper excitonic state corresponding to a lower excitonic dark state must occur at the very blue edge of the spectrum.

Apart from the distance and relative angles between pigments, Förster transfer also depends on the overlap between the emission spectrum of the donor and the absorption spectrum of the acceptor. The emission spectrum of a pigment is usually to the red of the absorption spectrum because of the Stokes shift, but even if we assume that the Stokes shift is zero, the amount of overlap between a line with width 100 cm^{-1} at position 14925 cm^{-1} and a similar line at 15200 cm^{-1} is negligible: for Gaussian lines the overlap factor is 0.02.

As a consequence, we may state that even if the lower excitonic state of a statistical dimer can be considered dark an excited monomer has no possible mechanism to transfer its energy to the higher excitonic state of that same dimer.

It is not immediately obvious that there could be no quenching dimers with small exciton splitting, but a moments reflection shows that the spectrum in Figure 2 gives also the correlation between lower state dipole moment and excitonic splitting: the lower half of the spectrum is the lower state dipole moment squared and the distance to the center of the spectrum just half the excitonic splitting, so small transition dipoles correlate directly with large exciton splitting.

Often dimers have a spectrum that is red-shifted compared to the monomer spectra, which would of course be helpful for

energy transfer from monomers, because it increases the overlap between monomer emission and highest excitonic state absorption, but on the other hand, the red shift can be taken as indicative for the coupling with a CT state,[25−27] so that those dimers which do get a considerable overlap are also those with the most charge-transfer character.

A possible way out of this dilemma is the introduction of inhomogeneous broadening mechanisms: inhomogeneous broadening is usually much larger than homogeneous broadening and could easily give us monomers which spectra overlap with upper excitonic states, but we will show in the next section that inhomogeneous broadening also has the effect of increasing lower excitonic state dipole strengths.

4. Inhomogeneous Broadening Effects

The starting point is again eq 2.11, but now we concentrate first on the integrals over the distribution functions $f(\epsilon)$. For a given set of angles and positions, the intensity $I(\upsilon)$ can be written as

$$I(\upsilon) = \frac{1}{2}\int_{-\infty}^{\infty} d\epsilon_1 \int_{-\infty}^{\infty} d\epsilon_2\, f(\epsilon_1)\, f(\epsilon_2)\, [I_+\delta(\upsilon - \epsilon_+) + I_-\delta(\upsilon - \epsilon_-)] \quad (4.1)$$

We introduce the following notation:[28]

$$\Delta = \frac{1}{2}|\epsilon_2 - \epsilon_1| \quad \text{and} \quad \Sigma = \frac{1}{2}|\epsilon_2 + \epsilon_1| \quad (4.2)$$

The new transition dipoles can then be written as

$$I_\pm = \mu^2\left[1 \pm \frac{V}{\sqrt{\Delta^2 + V^2}}\cos\theta\right] \quad (4.3)$$

and the corresponding energies are

$$\epsilon_\pm = \Sigma \pm \sqrt{\Delta^2 + V^2} \quad (4.4)$$

Furthermore a straightforward calculation gives the distribution of Σ and Δ as

$$P(\Sigma, \Delta) = \frac{1}{\pi\sigma^2}\exp[-(\epsilon_0 - \Sigma)^2/\sigma^2]\exp(-\Delta^2/\sigma^2) \quad (4.5)$$

The introduction of this result in eq 4.1 and subsequently performance of the integration of Σ gives

$$I(\upsilon) = \frac{\mu^2}{2\sqrt{\pi\sigma^2}}\int_{-\infty}^{\infty} d\Delta\, e^{-\Delta^2/\sigma^2}\left[\exp[-(\epsilon_0 - \upsilon + \sqrt{\Delta^2 + V^2})/\sigma^2]\left(1 + \frac{V}{\sqrt{\Delta^2 + V^2}}\cos\theta\right) + \exp[-(\epsilon_0 - \upsilon - \sqrt{\Delta^2 + V^2})/\sigma^2]\left(1 - \frac{V}{\sqrt{\Delta^2 + V^2}}\cos\theta\right)\right] \quad (4.6)$$

For $\Delta = 0$, we recover the stick spectrum; for not too large values of Δ, we can approximate the integral by

$$I(\upsilon) = \frac{1}{2}\mu^2\exp[-(\epsilon_0 - \upsilon + \sqrt{\sigma^2 + V^2})/\sigma^2] \times \left(1 + \frac{V}{\sqrt{\sigma^2 + V^2}}\cos\theta\right) + \frac{1}{2}\mu^2\exp[-(\epsilon_0 - \upsilon - \sqrt{\sigma^2 + V^2})/\sigma^2]\left(1 - \frac{V}{\sqrt{\sigma^2 + V^2}}\cos\theta\right) \quad (4.7)$$

In Figure 3, we have plotted the spectrum resulting from eq 4.6 as well as from (4.7) for an inhomogeneous broadening of 100 cm^{-1}. We took the special case where the transition dipoles are in the same direction and perpendicular to the vector connecting them, so that for the unperturbed system, the lower excitonic state is completely dark. We note that the spectrum can be reasonably well approximated by eq 4.7, that the exciton splitting is not equal to $2V$ but to $2(\sigma^2 + V^2)^{1/2}$, which differs substantially from $2V$, and finally that the lowest excitonic state acquired a considerable amount of dipole strength. Realistic values of σ are often higher. For $\sigma = 200$ cm^{-1}, we find that the lower excitonic state caries about 10% of the total oscillator strength. The effect of exchange narrowing that inhomogeneous broadening by diagonal disorder also shows is for a dimer not of great relevance.

In Figure 4, we show the spectrum resulting from averaging expression (4.6) over all possible orientations of the transition dipoles. As in Figure 2, the distance between the pigments is taken to be fixed at 1 nm. We note that in this case the diagonal disorder also has as one of its main effects a considerable increase in the intensity of the lower excitonic state.

Thus, we may state that although the introduction of diagonal disorder undoubtedly will increase the possibility of energy transfer from a monomeric pigment to the higher excitonic state of a quenching statistical dimer a side effect is, however, that the quenching properties of such a dimer are decreased.

Although the spectral effects of excitonic coupling on the systems studied so far are quite distinctive, ranging from observable excitonic splitting, as in figures 3, and 4 to enhancement of the red side of the spectrum for higher values of (in)homogeneous broadening, we do not expect to observe those effects in real systems. After all, the proportion of statistical pairs is small to begin with compared to the total number of absorbers, at least at low concentration, and furthermore, the distribution of distances also obscures the effect. Of course, when the concentration gets higher, the number of statistical pairs increases, but interaction with other pigments then also starts to play a role, because the likelihood of finding a trimer with relative distances smaller than 1 nm then also becomes appreciable. In the final section, we show some calculations of spectra of more concentrated systems by taking all interactions into account, here we show that even for ordered pairs with a distance distribution the specific spectral effects are diminished. To that end, we take the configuration described in the caption of Figure 3, but we vary the distance according to the Hertz distribution, eq 2.18.

The most probable distance for a given particle density is

$$\bar{R} = (2/3)^{1/3}R_0 \approx 0.87R_0 \quad (4.8)$$

and we choose the values for the simulation such that this distance is 1 nm. This accounts for the variance still found in statistical pairs within quenching distance of an excited monomer.

We note that this differs very little from the average distance for a given density, which can be written as

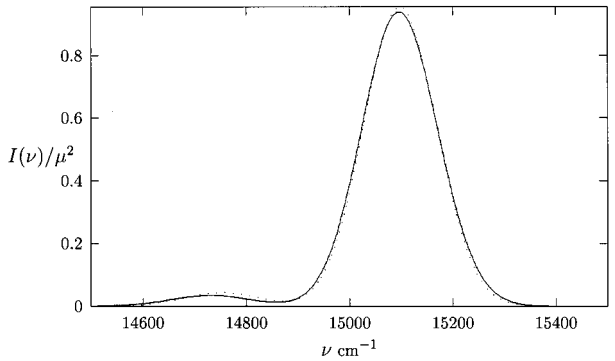

Figure 3. Disordered dimer spectrum calculated from eq 4.6 (solid line), and approximation eq 4.7 (dots). Parameters were chosen as follows: $\theta_1 = \theta_2 = \pi/2$, $\phi = 0$, $\mu = 5.6$ D, $R = 1$ nm, and $\sigma = 100$ cm^{-1}. The geometry of the dimer gives a lower excitonic state with no dipole strength in the absence of disorder. The full-width at half maximum (fwhm) of the monomer spectrum is $2.355\sigma \approx 236$ cm^{-1}.

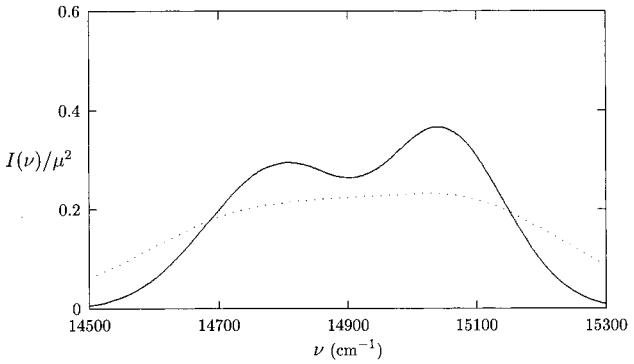

Figure 4. Inhomogeneously broadened spectrum of a statistical pair of chromophores. For the solid line, we used an inhomogeneous line width of 100 cm^{-1}; for the dotted line, 200 cm^{-1} was used. The latter is a more realistic value.

$$\langle R \rangle = R_0 \int_0^\infty \mathrm{d}x\, x^{1/3} \mathrm{e}^{-x} = R_0 \Gamma\left(\frac{4}{3}\right) \approx 0.89 R_0 \qquad (4.9)$$

In Figure 5, we show the spectrum resulting from a simulation where the distance was varied in accordance with the Hertz distribution, and where, in addition, we assumed a homogeneous line width of 100 cm^{-1} and an inhomogeneous width of 200 cm^{-1}. Also included is the spectrum of a monomeric pigment with the same broadening parameters. The dimer spectrum has become almost symmetrical and compared with the monomer spectrum is shifted toward the blue and slightly broader. Again there is considerable dipole strength at the red end of the spectrum.

In a subsequent paper,[10] we analyze spectra of erythrosin B in PVA film at varying concentrations, where apart from broadening a small blue shift can be observed at higher concentrations and which can therefore be attributed to the effect described here, although formation of oligomers can also contribute significantly.

The monomer spectrum displayed in Figure 5 was found by direct convolution of the Gaussian corresponding to the homogeneous broadening, and the Gaussian distribution of excitation energies. The result of this convolution is a Gaussian with width $(\sigma^2 + \sigma_h^2)^{1/2}$, where σ_h is the variance of the homogeneous Gaussian. The dimer spectrum is broader, even though there is a small exchange narrowing effect because of the distributed positions.

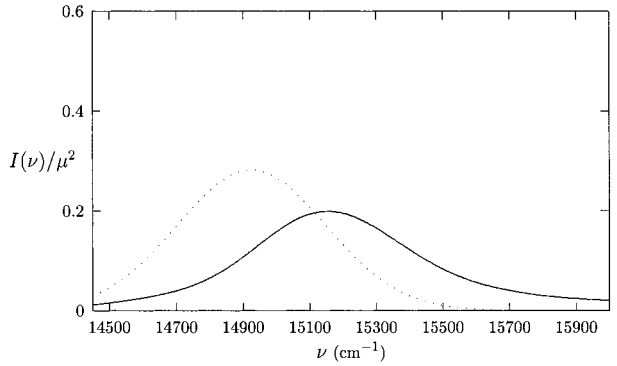

Figure 5. Spectrum of a statistical pair with fixed parallel orientation but positions distributed according to the Hertz distribution, eq 2.15. The most probable distance is chosen as 1 nm, and homogeneous (100 cm^{-1}) and inhomogeneous (200 cm^{-1}) broadening are included. Also shown (dotted) is the spectrum of a collection of monomers with the same values of homogeneous and inhomogeneous broadening parameters.

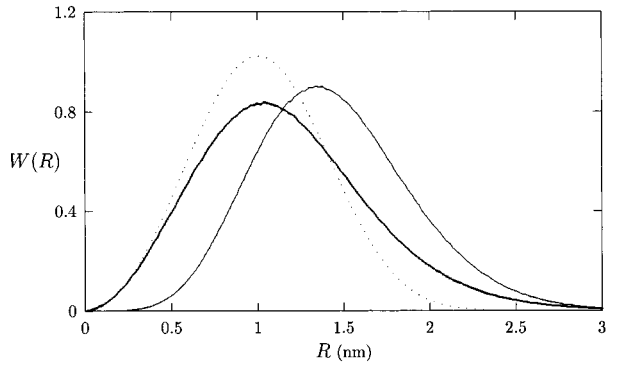

Figure 6. Normalized nearest neighbor distribution for randomly placed particles in a box. Also shown (dotted) is the Hertz distribution, eq 2.15, for $R_0 = 1.15$ nm. The thin solid line is the probability of finding a third pigment at distance R from the center of a nearest neighbor pair.

5. Spectral Effects

From the results of the previous section, it could be concluded that the spectral effects of the presence of statistical pairs is considerable. In all cases studied, the spectrum is asymmetric and there is a considerable blue shift, even if homogeneous and inhomogeneous broadening are included and if the distance distribution is taken into account. However, we also showed that the number of statistical pairs present in low concentration solution may be large enough to act as potential quenchers if an additional dark state is assumed, but the overwhelming majority of pigments will still occur in monomeric form and dominate the absorption spectrum.

The spectrum displayed in Figure 5 could be interpreted as the absorption spectrum of a collection of statistical pairs with preferred orientation. The spectral effects shown there, a blue shift, and extra broadening because of variations in relative positions could be observed for higher concentrations. However, for an average distance of 1 nm, the overall concentration is approximately 0.6 M, and consequently, a larger number of pigments can be found in the immediate proximity of a statistical dimer, thus rendering the statistical pair picture incomplete. In fact, on average, a third neighbor will be found at a distance of $\sqrt{2} \approx 1.4$ times the nearest neighbor distance (cf. Figure 6), which means that for a random system at a density such that the average distance is 1 nm the interaction strength with the next nearest neighbor, which is about 40% that of the nearest neighbor interaction, cannot be neglected. We could of course

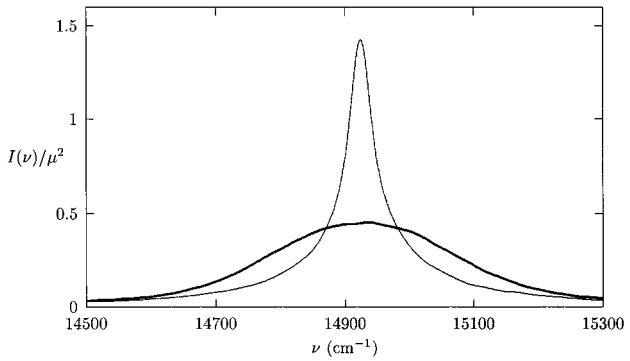

Figure 7. Absorption spectra for randomly distributed particles in a box. The particle density is 0.16 nm^{-3}, corresponding to a 0.27 M solution. Transition moments and excitation energies are like those in the other simulations. The thin solid curve is for an inhomogeneous broadening of zero, whereas the thick solid line has an inhomogeneous broadening of 100 cm^{-1}. The spectra were calculated with a small homogeneous broadening, 10 cm^{-1}, to speed up convergence.

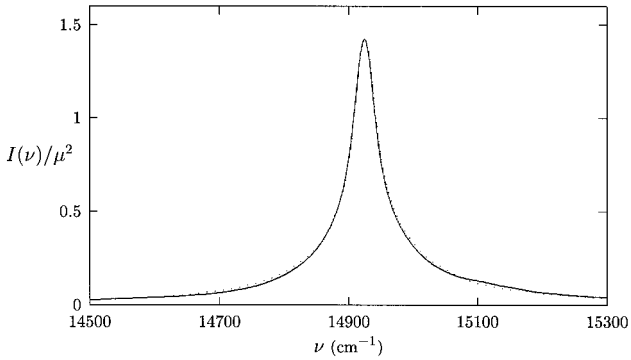

Figure 8. Absorption spectra for a random collection of pigments. The dotted spectrum is the same as the one displayed in the previous figure without inhomogeneous broadening. For the solid line spectrum, the additional assumption was made that pigments closer than 1 nm have parallel transition dipole moments. There is an extremely slight decrease on the red side of the spectrum and a corresponding slight increase on the blue side, in accordance with earlier results on statistical pairs.

consider trimers or tetramers, but that is hardly useful. It cannot be expected that they have a lowest excitonic state that is dark, and the ground state interaction will make it very unlikely that these oligomers are statistical in nature.

In this section, we show some results that could be found if systems were indeed completely random.

The simulations were done on 20 randomly positioned and oriented pigments in a cubic box of length 5 nm. The value of R_0 for this setup if 1.15 nm, so that the average distance and the most probable distance between nearest neighbors is $\approx$1 nm. In Figure 6, we show the nearest neighbor distribution function for this situation. It differs slightly from the Hertz distribution, because of boundary effects: for particles near a wall, there are fewer neighbors. The figure shows that this does not have appreciable effects on the most probable nearest neighbor position. Obviously, this could be improved using periodic boundary conditions, but for our purposes, that is hardly worthwhile.

For a large number of realizations ($N = 10^4$), we calculated the average absorption spectrum of such a system by calculating all excitonic interaction energies V_{ij} (cf. eq 2.2), diagionalizing the resulting Hamiltonian, and subsequently finding all excitonic states and their transition dipole moments. The result is displayed in Figure 7 for zero inhomogeneous broadening and for an inhomogeneous broadening of 100 cm^{-1}. We note that for zero inhomogeneous broadening there appears to be a large monomeric component to the spectrum, as evidenced by the sharp peak at the unperturbed transition frequency. There is no visible evidence for an enhancement at the blue side of the spectrum because of the presence of statistical pairs.

It can be inferred from Figure 6 that roughly half of the nearest neighbors at the given particle density are closer than 1 nm. To see if steric hindrance has observable effects on the absorption spectrum, we also performed a simulation where all particles closer than 1 nm are given the same orientation. The results are displayed in Figure 8 for a homogeneously broadened spectrum only. We used a small homogeneous broadening (10 cm^{-1}), mainly to speed up the convergence of the Monte Carlo calculation. Even for this small broadening, the enhancement on the blue side can hardly be noticed. Simulations with larger homogeneous broadening or additional inhomogeneous broadening do not show any difference with the spectra calculated without taking steric hindrance into account.

These results can easily be understood on the basis of the particle distribution function. As can be inferred from the results of the previous sections, a blue-shifted spectrum or enhancement of the blue side of the spectrum occurs for dimers with a preferred parallel orientation of the dipole moments or statistical pairs, where the contribution of blue-shifted spectra is still predominant over the red-shifted spectra. A direct calculation shows that even for the relatively high concentrations considered here the number of pairs of pigments closer than 1.5 nm (for larger distances, the excitonic interaction becomes too small to give appreciable effects) still does not exceed more than 10% of the total number of pairs. Even if we use maximal enhancement of these pairs by choosing them to have parallel transition moment, the contribution is negligible.

6. Conclusions

The aim of this paper is twofold: to give an estimate of the number of potential quenchers in the neighborhood of an excited chromophore and to show what the spectral effects of those quenchers are on the observed absorption spectrum.

Although a perfectly ordered dimer with a dark lower excitonic state could potentially act as a quencher, we have shown, on the basis of the Hertz distribution, that such pairs are far to few in number if homogeneous and inhomogeneous broadening are taken into account or (restricted) distributions over the relative orientations and distances. For higher concentrations, where the number of potential quenchers increases, the interaction with other nearby pigments starts to play a role, and the probability of finding a lowest excitonic dark state again decreases.

Spectroscopically the presence of quenching pairs will not be noticed, at least not in ordinary absorption spectroscopy. The results of the previous section indicate that the absorption spectrum of a collection of pigments will mainly just be broadened at higher concentrations because of excitonic interactions, and the characteristic blue shift of the statistical pairs contributes insufficient to give an observable effect.

Appendix

Derivation of eq 3.6. The starting point of the derivation is expression (3.5). To make the derivation more readable, we introduce the following dimersionless variables:

$$e_{\pm} = \frac{e_{\pm} - \epsilon_0}{V_0} = \pm(\sin\theta_1 \sin\theta_2 \cos\phi - 2\cos\theta_1 \cos\theta_2)\ \mathrm{sign}\ V \quad (A.1)$$

and

$$i_{\pm} = \frac{I_{\pm}}{\mu^2} - 1 = \pm(\sin\theta_1 \sin\theta_2 \cos\phi + \cos\theta_1 \cos\theta_2) \quad (A.2)$$

where we note that $|e_{\pm}| \leq 2$ and $|i_{\pm}| \leq 1$. Introducing $\theta_i = x_i$, then yields

$$e_+ = -e_- = \sqrt{1 - x_1^2}\sqrt{1 - x_2^2}\cos\phi - 2x_1x_2 \quad (A.3)$$

and

$$i_+ = -i_- = \sqrt{1 - x_1^2}\sqrt{1 - x_2^2}\cos\phi + x_1x_2 \quad (A.4)$$

Equation 3.5 can then be rewritten as

$$P(i, e) = \frac{\epsilon\bar{R}^3}{16\pi\mu^4 V_0}\int_0^{2\pi} d\phi \int_{-1}^{1} \mathrm{d}x_1 \int_{-1}^{1} \mathrm{d}x_2\, (\delta(e - e_+)\delta(i - i_+) + \delta(e - e_-)\delta(i - i_-)) \quad (A.5)$$

where we also wrote $e = (\upsilon - \epsilon_0)/V_0$ and $i = I/\mu^2 - 1$.

Equation 2.13 can be expressed as

$$I(\upsilon) = \mu^2 \int_{-1}^{1} \mathrm{d}i\ (i + 1)P(i, e) \quad (A.6)$$

Integration over ϕ is straightforward and gives

$$P(i, e) = \frac{1}{8\pi\mu^2 V_0}\int_{-1}^{1} \mathrm{d}x_1 \int_{-1}^{1} \mathrm{d}x_2 \times \left[\frac{\delta(e - i + 3x_1x_2)}{\sqrt{(1 - x_1^2)(1 - x_2^2) - (i - x_1x_2)^2}} + \frac{\delta(e - i - 3x_1x_2)}{\sqrt{(1 - x_1^2)(1 - x_2^2) - (i + x_1x_2)^2}}\right] \quad (A.7)$$

where the values of i have to be such that the arguments of the square roots in these expressions are positive. Outside that range, the result is zero. Note that both terms are in fact equal: a simple change of variables, for instance $x_2 \rightarrow -x_2$ in the second term, proves this. Subsequently, integrating over x_2 gives

$$P(i, e) = \frac{1}{2\pi\mu^2 V_0}\int_0^1 \mathrm{d}x_1 \frac{1}{\sqrt{(1 - x_1^2)(9x_1^2 - (e - i)^2) - x_1^2(2i + e)^2}} \quad (A.8)$$

again with the requirement that the argument of the square root is positive. This restricts the integration interval of x_1 for specific values of i and e. We also used that the integrand is symmetric in x_1.

Although it is possible to get analytical expressions in terms of elliptic functions for this integral, these are rather complicated. However, in view of eq A.6, we only need

$$\langle i + 1\rangle_e = \int_{-1}^{1} \mathrm{d}i\ iP(i, e) + \int_{-1}^{1} \mathrm{d}i\ P(i, e) = \int_{-1}^{1} \mathrm{d}i\ iP(i, e) + P(e) \quad (A.9)$$

To calculate the integrals in eq A.9, we rewrite the square root in eq A.8 as a function of i:

$$\sqrt{(1 - x_1^2)(9x_1^2 - (e - i)^2) - x_1^2(2i + e)^2} = \sqrt{ai^2 + bi + c} \quad (A.10)$$

with

$$a = -3x_1^2 - 1, \quad b = -6ex_1^2 + 2e, \quad \text{and } c = -9x_1^4 + 9x_1^2 - e^2 \quad (A.11)$$

First we note that

$$a \pm b + c = -[3x_1^2 \mp 1 \pm e]^2 < 0 \quad (A.12)$$

This means that at the boundaries $i \pm 1$ the argument of the square root in eq A.10 is negative for all values of x_1.

Furthermore $b^2 - 4ac$ can be written as

$$b^2 - 4ac = -36x_1^2(x_1^2 - 1)(3x_1^2 - e^2 + 1) \quad (A.13)$$

It is easy to see that for $|e| < 1$ this discriminant is larger than zero for all values of $0 < x_1 < 1$, whereas for $1 < |e| < 2$ it is only larger than zero in the interval $x_i \in \{[(e^2 - 1)/3]^{1/2}, 1\}$.

Equations A.12 and A.13 imply that the effective boundaries of the integration over i are $\{-b \pm [(b^2 - 4ac)]^{1/2}\}/2a$.

Equation A.9 can now be written as

$$\langle i + 1\rangle_e = \frac{1}{2\pi\mu^2 V_0}\int \mathrm{d}x_1 \int \mathrm{d}i\, \frac{i + 1}{\sqrt{ai^2 + bi + c}} \quad (A.14)$$

The integration over i can be performed[29] and gives upon introduction of the integration boundaries and some straightforward algebraic manipulations

$$\int \mathrm{d}i\, \frac{i + 1}{\sqrt{ai^2 + bi + c}} = \pi\left[\frac{2e}{(3x_1^2 + 1)^{3/2}} + \frac{1 - e}{(3x_1^2 + 1)^{1/2}}\right] \quad (A.15)$$

The remaining integral can be written as

$$\langle i + 1\rangle_e = \frac{1}{\mu^2 V_0}\left[e\int_{\alpha}^{1} \mathrm{d}x\, (1 + 3x^2)^{-3/2} + \frac{1}{2}(1 - e)\int_{\alpha}^{1} \mathrm{d}x\, (1 + 3x^2)^{-1/2}\right] \quad (A.16)$$

with $\alpha = 0$ if $|e| < 1$ and $\alpha = [(e^2 - 1)/3]^{1/2}$ if $1 < |e| < 2$. Both integrals are standard,[29] and the result is given in the main text as eqs 3.6 and 3.7.

References and Notes

(1) Kühlbrandt, W.; Wang, D. N.; Fujiyoshi, Y. *Nature* **1994**, *367*, 614.

(2) Gerhardt, H. In *Dye Lasers*; Schäfer, F. P., Ed.; Springer−Verlag: Berlin, 1999; pp 121−137.

(3) Watson, W. F.; Livingston, R. *J. Chem. Phys.* **1950**, *18*, 802.

(4) Beddard, G. S.; Porter, G. *Nature* **1976**, *260*, 366.

(5) Ide, J. P.; Klug, D. R.; Kühlbrandt, W.; Georgi, L.; Porter, G. *Biochim. Biophys. Acta* **1987**, *983*, 384.

(6) Van Zandvoort, M. A. M. J.; Wróbel, D.; Scholten, A. J.; de Jager, D.; van Ginkel, G.; Levine, Y. K. *Photochem. Photobiol.* **1993**, *58*, 600.

(7) Van Zandvoort, M. A. M. J.; Wróbel, D.; Lettinga, P.; van Ginkel, G.; Levine, Y. K. *Photochem. Photobiol.* **1995**, *62*, 279.

(8) Knox, R. S. *J. Phys. Chem.* **1994**, *98*, 7270.

(9) Kroon, J. M.; Sudholter, E. J. R.; Wienke, J.; Koehorst, R. B. M.; Savenije, T. J.; Schaafsma, T. J. In *Proceedings of the 13th European Photovoltaic Solar Energy Conference*; 1995; pp 1295−1298.

(10) Stomphorst, R. G.; van Zandvoort, M. A. M. J.; Sieval, A.; Zuilhof, H.; Vergeldt, F. J.; Schaafsma, T. J.; van der Zwan, G. *J. Phys. Chem. A* **2001**, *105*, 4235.
(11) Hertz, P. *Math. Ann.* **1908**, *67*, 387.
(12) Beekman, L. M.; Steffen, M.; van Stokkum, I.; Hunter, C. N.; Boxer, S. G.; van Grondelle, R. *J. Phys. Chem. B* **1997**, *101*, 7284.
(13) Beekman, L. M.; Frese, R. N.; Fowler, G. J. S.; van Stokkum, I.; Hunter, C. N.; van Grondelle, R. *J. Phys. Chem. B* **1997**, *101*, 7293.
(14) Boxer, S. G. In *Biophysical techniques in photosynthesis*; Amesz, J., Hoff, A. J., Eds.; Kluwer Academic Publishers: Amsterdam, The Netherlands, 1996; pp 177−189.
(15) Remacle, F.; Levine, R. D. *J. Phys. Chem. A* **2000**, *104*, 2341.
(16) Van der Zwan, G.; Hynes, J. T. *J. Phys. Chem.* **1985**, *89*, 4181.
(17) Kim, H. J.; Hynes, J. T. *J. Chem. Phys.* **1990**, *93*, 5194.
(18) Kim, H. J.; Hynes, J. T. *J. Chem. Phys.* **1990**, *93*, 5211.
(19) Kim, H. J.; Hynes, J. T. *J. Chem. Phys.* **1992**, *96*, 5088.
(20) Gehlen, J. N.; Chandler, D.; Kim, H. J.; Hynes, J. T. *J. Phys. Chem.* **1992**, *96*, 1748.
(21) Koolhaas, M. H. C.; van der Zwan, G.; van Mourik, F.; van Grondelle, R. *Biophys. J.* **1997**, *72*, 1828.
(22) Chandrasekhar, S. In *Selected papers on noise and stochastic processes*; Wax, M., Ed.; Dover Publications, Inc.: New York, 1954; pp. 2−88.
(23) Georgakopoulou, S.; Frese, R. N.; Koolhaas, M. H. C.; Cogdell, R.; van Grondelle, R.; van der Zwan, G. *Biophys. J.* Submitted, 2000.
(24) Press, W. H.; Teukolsky, S. A.; Vetterling, W. T.; Flannery, B. P. *Numerical Recipes in C*; Cambridge University Press: Cambridge, U.K., 1992; Chapter 7.
(25) Warshel, A.; Parson, W. W. *J. Am. Chem. Soc.* **1987**, *109*, 6143.
(26) Parson, W. W.; Warshel, A. *J. Am. Chem. Soc.* **1987**, *109*, 6153.
(27) Laguitton−Pasquier, H.; Pansu, R.; Chauvet, J.-P.; Collet, A.; Faure, J.; Lapouyade, R. *Chem. Phys.* **1996**, *212*, 437.
(28) Koolhaas, M. H. C.; van Mourik, F.; van der Zwan, G.; van Grondelle, R. *J. Lumin.* **1994**, *60*/*61*, 515.
(29) Gradshteyn, I. S.; Ryzhik, I. M. *Tables of Integrals, Series and Products*; Academic Press: London, 1980.